Phonon recycling in ion-doped lasers

Jedo Kim and Massoud Kaviany[a)]
Department of Mechanical Engineering, University of Michigan, Ann Arbor, Michigan 48109-2125, USA

(Received 16 June 2009; accepted 30 July 2009; published online 19 August 2009)

Phonon emission is an energy-conversion efficiency loss in photonic transition processes. Phonon recycling by the anti-Stokes cooling results in a lower operating temperature. Transmitted optical phonons cross heterogeneous boundary and the upconverted acoustic phonons contribute to higher occupancy of the optical phonon and increase the second-order transition rate. Optimization of phonon spectra makes upconversion favorable. We present theoretical study and quantitative efficiency results for phonon recycling in Yb^{3+} doped yttria alumina garnet lasing layer and its adjacent Yb^{3+}:ZrF_2 cooling layers and examine the thermodynamic limits. It is predicted that 30% of emitted phonons are recycled and further improvement is possible. © *2009 American Institute of Physics*. [DOI: 10.1063/1.3207824]

Energy recycling in photonic devices is promising (e.g., high-power lasers, where the laser inefficiency is critical[1]). Laser inefficiency stems from quantum defects (emitted photon energy is lower than that absorbed, $\hbar\omega_{\mathrm{ph,P}} > \hbar\omega_{\mathrm{ph},L}$) and emitted phonons carry away excess entropy produced during absorption of multimode pumping photons. The second law requires that emitted phonons have higher entropy compared to photons. Thus, in high-power lasers, elaborate cooling systems are unavoidable and hinder development of efficient, portable units. Recent efforts on radiation-balanced laser systems have provided alternatives to mechanical cooling systems. However, limited photon wavelength contrast of single-crystal laser medium used[2,3] poses a significant challenge. In this letter, we present theoretical development and prediction of phonon recycling (phonon excitation and recombination) in a multilayer ion-doped laser using the anti-Stokes luminescence. Anti-Stokes luminescence has cooled ion-doped solids from room temperature to 208 K and its theory has been advanced recently.[4–8] Anti-Stokes luminescence is reverse of the quantum defect (i.e., $\hbar\omega_{\mathrm{ph,sp}} > \hbar\omega_{\mathrm{ph,P}}$) and the excess entropy is removed by multimode incoherent spontaneous photons. The phonon-assisted photon absorption rate strongly depends on the high-energy phonon occupation, making it inefficient at low temperatures.[8,9] Conversely, at moderate to high temperatures, the high-energy phonons are more accessible. Phonon recycling in ion-doped lasers uses this by absorbing the high-energy phonons created in the lasing layer to drive the antiStokes process in the adjacent cooling layers as shown by the energy flow diagram in Fig. 1. Thus, phonon recycling involves dynamics of the three energy carrier [photon (ph), electron (e), and phonon (p)] interactions within and across two heterogeneous layers. The second-order transition process is treated using the Fermi golden rule and the final form of the transition rate is[8]

$$\dot{\gamma}_{\text{ph-}e\text{-}p} = \frac{\pi\hbar}{2\epsilon_o m}(\boldsymbol{s}_{\mathrm{ph},i}\cdot\boldsymbol{\mu}_{\text{ph-}e})^2\varphi'^2_{d,\mathrm{O}}D_p(E_{p,\mathrm{O}}) \times\frac{f_p(E_{p,\mathrm{O}})}{E^3_{p,\mathrm{O}}}\frac{L}{u_{\mathrm{ph}}}\frac{Q_{\mathrm{ph,P}}-Q_{\mathrm{ph},a}}{n_{d,\mathrm{C}}V}, \quad (1)$$

where m is the reduced mass of the host atomic pair, $\boldsymbol{s}_{\mathrm{ph},i}$ is the polarization vector, $\boldsymbol{\mu}_{\text{ph-}e}$ is electronic transition dipole moment vector, $\varphi'_{e\text{-}p,\mathrm{O}}$ is optical-phonon deformation potential, $D_p(E_{p,\mathrm{O}})$ is phonon density of states (DOS) of phonon having energy $E_{p,\mathrm{O}}$, f_p is phonon distribution function, L is photon transit length, u_{ph} is speed of light, and $(Q_{\mathrm{ph,P}}-Q_{\mathrm{ph},a})/n_{d,\mathrm{C}}V$ represents photon intensity per dopant ion. So, the phonon-assisted photon transition rate is a function of atomic properties of the dopant ion and host, which are optimized for desired performance.[8]

In ion-doped lasers, phonons are emitted in the lasing layer by temperature-independent rapid single-phonon decay and by temperature-dependent multiphonon decay. These nonequilibrium phonon distribution drive phonon propagation to the adjacent cooling layer. The propagation process involves acoustic-optical phonon up- and downconversion (three-phonon processes)[10,11] and optical and acoustic-phonon transmission, which are influenced by the phonon spectrum of both layers.[12,13] Figure 2(a) shows the Debye–

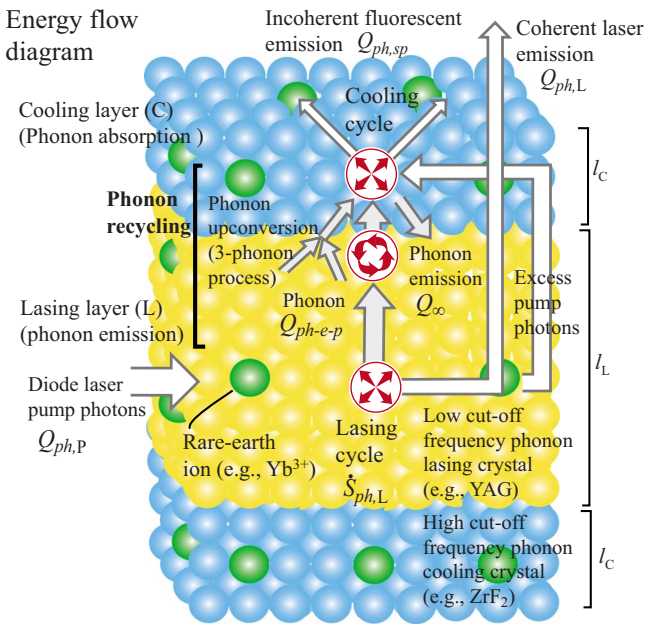

FIG. 1. (Color online) The energy-flow diagram, interactions among ions, photons, and phonons. Photon (clear arrow) and phonon (gray arrow) energy flows and heat flow diagram.

a)Electronic mail: kaviany@umich.edu.

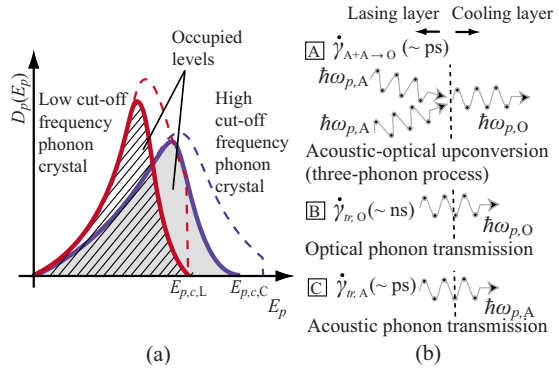

FIG. 2. (Color online) (a) Overlap of phonon DOS (Debye–Gaussian model) for low (red) and high (blue) cut-off frequency crystals (not to scale). Filled areas under the curve are the occupied phonon states at a given temperature. Saturation of low frequency phonons in the cooling layer makes upconversion favorable and transmission of phonons are needed from the lasing layer. (b) The three-phonon transfer mechanisms.

Gaussian model for $D_p(E_p)$ (Ref. 8) with low cut-off energy $(E_{p,c,L})$ phonon host in the lasing and high cut-off $(E_{p,c,C})$ in cooling layer. The three phonon processes involved in heat transfer across layers are shown in Fig. 2(b). Note that the figure is not to scale, and the phonon DOS integrates to $3N$, where N is the number of atoms, so depending on the cut-off phonon energies, the curves move up or down. The shaded areas under the curves in Fig. 2(a) represent occupied phonon levels at a given temperature and are the product of phonon DOS and the boson distribution function. When $E_{p,c,L} < E_{p,c,C}$, the average value of $D_p(E_p)$ is higher in the lasing layer, and for a given energy, phonons occupy the lower energy states because of their higher availability. In contrast, for the cooling layer, the value of $D_p(E_p)$ is lower but extends further into the high-energy regime. Thus, equilibrium phonons occupy higher energy states. During laser operation, generated phonons begin to occupy higher energy states in the lasing laser and create energy nonequilibrium between the lasing and cooling layers. In crossing the interface, most low-energy phonon states are already occupied in the cooling layer. Thus, for phonons to propagate into the cooling layer, among the three-phonon processes, the acoustic-optical phonons upconversion process becomes favorable. The added high-energy phonons in the cooling layer are used in the phonon-assisted absorption (anti-Stokes absorption).

Because of phonon transmission and upconversion processes, equilibrium f_p^o used in Refs. 7 and 8 is no longer valid in calculating the transition rate involving phonon recycling. Calculation of the exact nonequilibrium distribution is very challenging. However, we calculate the time scales for each processes to identify the bottleneck mechanism. It is then reasonable to assume the nonbottleneck processes as equilibria. For example, acoustic phonon thermalization and the upconversion of two acoustic phonons to one optical phonon are of the order of picosecond.[10,11,13] However, due to their low speed, the optical phonon transmission is expected to have time scale of the order of 10 ns,[14] for submillimeter travel distance. Thus, the bottleneck process is identified as optical phonon transmission. Therefore, deviation from f_p^o for transmitted optical phonons is accounted for by introducing a transmission coefficient $\tau_{p,tr,O}$, while equilibrium distribution is used for the three-phonon upconversion process. These

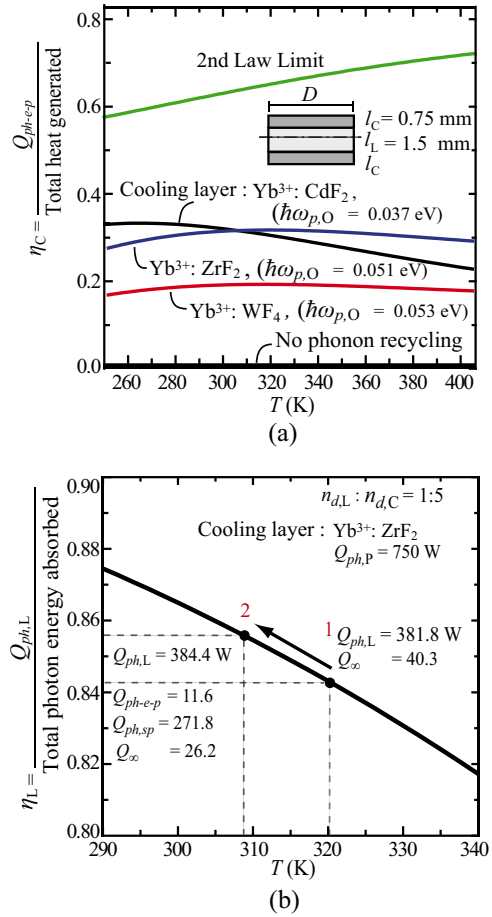

FIG. 3. (Color online) (a) Phonon-cooling performance as a function of temperature for phonon-recycled ion-doped laser using three different cooling crystals. D=1 cm, l_L=1.5 mm, and l_C=0.75 mm, Yb^{3+} doped disk is used, and emission spectra of Yb^{3+}:ZBLANP is used to calculate the spontaneous emission peak of anti-Stokes cooling (Refs. 21 and 22). The second law limit of the anti-Stokes cooling is also shown (Refs. 19 and 20). (b) Laser operation conditions as a function of temperature with (2) and without (1) phonon recycling. The reduced cooling load corresponds to a reduced laser crystal temperature and moves the operating condition to 2.

treatments of the nonequilibrium phonon populations give

$$f_p = f_p^o(E_{p,O}) + \tau_{p,tr,O} f_p^o(E_{p,O}) + f_p^o(E_{p,A_1}) f_p^o(E_{p,A_2}) \times [f_p^o(E_{p,O}) + 1], \quad (2)$$

where $f_p^o(E_{p,A_1})$ and $f_p^o(E_{p,A_1})$ are distributions of any two acoustic phonon energies, which can be annihilated to create one optical phonon of energy $E_{p,O}$ and must be allowed by the phonon dispersion relation and momentum conservation.[10] Note that as the time-scale contrast decreases, the population deviates from equilibrium, resulting in a lower occupation number for the three-phonon process.

The phonon recycling transition rates appear in macroscopic energy equation, as $Q_{\text{ph-}e\text{-}p} = n_{d,C} \dot{\gamma}_{\text{ph-}e\text{-}p} V$, along with energy conversion $\dot{S}$ energy transfer Q, for steady-state behavior of ion-doped laser layer and its adjacent anti-Stokes cooling layer. Figure 3(a) shows cooling efficiency η_C (heat removed by the anti-Stokes cooling/total heat generated by lasing) as a function of temperature, for three different cooling crystals (ZrF_2, CdF_2, and WF_2) with dopant Yb^{3+}, and Yb^{3+}: yttria alumina garnet (Yb^{3+}:YAG) as lasing crystal. The cooling crystal hosts are selected for their high, moderate, and low peak phonon energies, and the method for

evaluating the necessary atomic quantities in Eq. (1) are given in Ref. 8 and validity of the electron-phonon interaction potential used there has been confirmed in Ref. 15. The pumping, laser (Yb^{3+}:YAG), and spontaneous emission (Yb^{3+}:ZBLANP) (ZrF_4-BaF_2-LaF_3-AlF_3-NaF-PbF_2) wavelengths are: $\lambda_{ph,P}=998$ nm, $\lambda_{ph,L}=1030$ nm, and $\lambda_{ph,sp}=975$ nm. The results shows that for ZrF_2 (optical phonon energy of 0.051 eV), phonon recycling rate peaks at the conventional laser operation temperatures $T_L=300$ to 325 K, with approximately 30% of phonons recycled. At low temperatures, the anti-Stokes cooling rate rapidly diminishes, while the temperature-independent, rapid single-phonon decay remains constant. At high temperatures, the anti-Stokes cooling rate increases, and temperature-dependent multiphonon decay dominates over all other mechanisms and decreases the phonon recycling rate. For crystals with low optical phonon energy, e.g., CdF_2, phonon recycling peaks at lower temperatures, but decreases rapidly at high temperatures (due to low optical phonon transmission rate). In contrast, high phonon energy crystals such as WF_4 result in a much lower phonon recycling rate (due to their rather large reduced mass and lower phonon occupancy number). In practice, experiments use combination of materials to achieve maximum cooling because of statistical distribution of the spontaneous emission spectrum resulting from various defects and impurities.[9,16] In Fig. 3(b), variation in laser efficiency η_L (laser emission/total absorption) is shown for a laser system as a function of temperature. The laser with no phonon recycling is pumped by $Q_{ph,P}=750$ W diode laser, while producing $Q_{ph,L}=381.8$ W laser emission and $Q_\infty=40.3$ W of heat (rest of energy is lost without being absorbed).[21] With added cooling layers of the same volume and having five times the dopant concentration, we predict $Q_{ph\text{-}e\text{-}p}=12.8$ W of heat is removed by the phonon recycling producing $Q_{ph,sp}=302.2$ W of spontaneous emission. When the same external cooling unit is used, for example, $Q_\infty=40.3$ W, the reduced cooling load translates to 12 K lower crystal operating temperature, moving the operating conditions to slightly higher laser efficiency. Alternatively, for the same operating temperature, the phonon-recycled laser requires 30% less cooling resulting in a significant decrease in the cooling unit and may allow air cooled units for portability. The thermodynamic limit is found by applying the second law to the phonon-recycled laser.[17,18] The entropy generation and removal rates are evaluated using the corresponding Q_i/T_i. To find the equilibrium temperatures of the photon source, the thermodynamics of radiation is used and we find temperatures of 11 000, 44 000, and 4500 K for diode laser T_P, laser T_L, and spontaneous emission $T_{ph,sp}$, respectively, while the entropy of phonons is evaluated at the laser crystal temperature T.[19,20] The result is plotted in Fig. 3(a). This shows that phonon recycling satisfies the second law and is open to future improvement (removing inefficiencies in carrier interactions).

In summary, synergetic effect of introducing the anti-Stokes cooling in ion-doped lasing through phonon recycling is proposed and the predicted performances presented. The lasing and cooling kinetics are governed by atomic quantities comprising the carrier interaction rates, which then are introduced in the macroscopic energy equation. Phonon transmission between the adjacent lasing and upconversion cooling layer are discussed and included in the nonequilibrium phonon occupancy. For the example considered, the increased phonon population enhances the anti-Stokes cooling rate resulting in 30% phonon recycling and a slight improvement in laser efficiency is predicted when using the same cooling unit.

[1] A. Ikesue and Y. L. Aung, Nat. Photonics **2**, 721 (2008).
[2] S. R. Bowman, IEEE J. Quantum Electron. **35**, 115 (1999).
[3] S. R. Bowman, S. P. O'Connor, and S. Biswal, IEEE J. Quantum Electron. **41**, 1510 (2005).
[4] J. Thiede, J. Distel, S. R. Greenfield, and R. I. Epstein, Appl. Phys. Lett. **86**, 154107 (2005).
[5] R. Epstein, M. I. Buchwald, and B. C. Edwards, Nature (London) **377**, 500 (1995).
[6] J. Fernandez, A. J. Garcia-Adeva, and R. Balda, Phys. Rev. Lett. **97**, 033001 (2006).
[7] X. L. Ruan and M. Kaviany, Phys. Rev. B **73**, 155422 (2006).
[8] J. Kim, A. Kapoor, and M. Kaviany, Phys. Rev. B **77**, 115127 (2008).
[9] M. P. Hehlen, R. I. Epstein, and H. Inoue, Phys. Rev. B **75**, 144302 (2007).
[10] J. Ziman, *Electrons and Phonons* (Oxford University Press, London, 1962).
[11] G. P. Srivastava, *The Physics of Phonons* (Adam Hilger, Bristol, 1990).
[12] E. Swartz and R. Pohl, Rev. Mod. Phys. **61**, 605 (1989).
[13] M. Kaviany, *Heat Transfer Physics* (Cambridge University Press, Cambridge, 2008).
[14] X. F. Pang and Y. P. Feng, *Quantum Mechanics in Nonlinear Systems* (World Scientific, Singapore, 2005).
[15] J. Kim and M. Kaviany, Phys. Rev. B **79**, 054103 (2009).
[16] G. Lei, J. E. Anderson, M. I. Buchwald, B. C. Edwards, R. I. Epstein, M. T. Murtagh, and G. Sigel, IEEE J. Quantum Electron. **34**, 1839 (1998).
[17] L. Landau, J. Phys. USSR (Moscow) **10**, 503 (1946).
[18] P. T. Landsberg and G. Tonge, J. Appl. Phys. **51**, R1 (1980).
[19] C. E. Mungan, J. Opt. Soc. Am. B **20**, 1075 (2003).
[20] X. L. Ruan, S. C. Rand, and M. Kaviany, Phys. Rev. B **75**, 214304 (2007).
[21] W. T. Silfvast, *Laser Fundamentals*, 2nd ed. (Cambridge University Press, Cambridge, 2004).
[22] G. Lei, J. E. Anderson, M. I. Buchwald, B. C. Edwards, and R. I. Epstein, Phys. Rev. B **57**, 7673 (1998).